Resonating properties of passive spherical optical microcavities

Wen Li (李 文) and Ruopeng Wang (王若鹏)

Department of Physics and State Key Laboratory for Mesoscopic Physics, Peking University, Beijing 100871

Received November 4, 2003

As an optically pumped device, the lasing characteristics of a spherical microcavity laser depend on the optical pumping processes. These characteristics can be described in term of the Q factor and the optical field distribution in a microsphere. We derived analytical expressions and carried out numerical calculation for Q factor and optical field. The Q factor is found to be oscillatory functions of the radius of a microsphere and the pumping wavelength, and the pumping efficiency for a resonating microsphere is much higher than that for an anti-resonating microsphere. Using tunable lasers as pumping sources is suggested in order to achieve a higher pumping efficiency. Numerical calculation on optical field distribution in spherical microcavities shows that a well focused Gaussian beam is a suitable incident wave for cavity quantum electrodynamics experiments in which strong confinement of optical field in the center of a microsphere is requested, but higher order spherical wave should be used instead for exciting whispering-gallery-mode (WGM) microsphere lasers, for the purpose of favoring optical energy transferring to WGM in optical microspheres.

OCIS codes: 140.5560, 140.4780, 260.2160.

Microlasers with high Q factor spherical resonators are attractive systems both for cavity quantum electrodynamics researches[1−3] and for optoelectronics applications[4,5]. Due to the specific structure of microsphere lasers, the optical pumping is used for these devices. As an optically pumped device, the lasing characteristics of a microsphere laser depend not only on its behavior in the light emitting process, but also on its behavior in the optical pumping processes, in which a microsphere acts as a passive optical cavity. In fact, the optical gain in the lasing spectral range of a microsphere laser is determined by the intensity and the distribution of the pumping optical field in the microsphere. Many theoretical analyses have been done in the distribution of the optical field in dielectric sphere when it is excited by incident plane wave[6]. We studied the resonating properties of a passive microsphere through the solution of the optical field distribution when it is under optical pumping. By carefully analyzing the resonating properties of passive microspheres and choosing suitable optical pumping mode, the efficiency of microlasers with spherical resonators could be considerably improved.

The efficiency of the optical pumping process can be defined as the ratio between the optical power absorbed by a microsphere $P_{\rm abs}$ and the incident optical power $P_{\rm inc}$

$$\eta = \frac{P_{\rm abs}}{P_{\rm inc}}. \tag{1}$$

To calculate the incident optical power, we may separate an optical field into two parts

$$\mathbf{E}(\mathbf{r},t) = \mathbf{E}^{(+)}(\mathbf{r},t) + \mathbf{E}^{(-)}(\mathbf{r},t). \tag{2}$$

Each of them satisfies the Maxwell equations in free space, and has the asymptotical behaviors at the limit $|\mathbf{r}| \to \infty$ as

$$\mathbf{E}^{(+)}(\mathbf{r},t) \sim \frac{\mathrm{e}^{ik_0|\mathbf{r}|}}{|\mathbf{r}|}, \quad \mathbf{E}^{(-)}(\mathbf{r},t) \sim \frac{\mathrm{e}^{-ik_0|\mathbf{r}|}}{|\mathbf{r}|}, \tag{3}$$

where k_0 is the modulus of the wave vector in vacuum.

We also request that distribution of $\mathbf{E}^{(-)}(\mathbf{r},t)$ in free space is determined only by the pumping source. $\mathbf{E}^{(-)}(\mathbf{r},t)$ is the so-called incident optical wave, and $\mathbf{E}^{(+)}(\mathbf{r},t)$ the outgoing or diffracted optical wave. The incident optical power then can be calculated by integrating the Poynting's vector of the incident wave over the surface of an optical microsphere

$$P_{\rm inc} = \frac{1}{2}\oint_S \mathrm{Re}(\mathbf{H}^{(-)*} \times \mathbf{E}^{(-)}) \cdot \mathrm{d}\mathbf{S}. \tag{4}$$

The calculation of the optical power absorbed by a microsphere is straightforward. For a homogeneous microsphere, we have the expression of absorbed power from Poynting theorem[7]

$$P_{\rm abs} = \frac{\omega \mathrm{Im}(n^2)}{\mathrm{Re}(n^2)} \mathrm{Re}[\int_V \frac{1}{4}\mathbf{E}^* \cdot \mathbf{D}\mathrm{d}v], \tag{5}$$

where n is the complex refractive index of the microsphere, and the integral is taken over the volume of the microsphere.

On the other hand, an optical resonator is described by a Q factor which is defined as 2π times the ratio between the electrical energy stored in a microsphere and the optical energy lost in one cycle. At a steady state, the rate optical energy loss must equal the incident optical power. So we have

$$Q = \frac{\omega \mathrm{Re}[\int_V \mathbf{E}^* \cdot \mathbf{D}\mathrm{d}v]}{2\mathrm{Re}[\oint_S (\mathbf{H}^{(-)*} \times \mathbf{E}^{(-)}) \cdot \mathrm{d}\mathbf{S}]}. \tag{6}$$

According to expressions (4)−(6), we have then

$$\eta = \frac{\mathrm{Im}(n^2)}{\mathrm{Re}(n^2)} Q. \tag{7}$$

Evidently, the optical pumping efficiency depends not only on the complex refractive index n, but also on the

resonating property of microspheres. As can be seen from Eq. (7), the Q factor is a suitable parameter for describing the resonating property of microspheres.

To calculate the Q factor of a microsphere, we need the optical field distribution within a microsphere for a given incident wave. It is convenient to use the vector potential $\mathbf{A}(\mathbf{r},t)$ to describe the optical field. By using the Coulomb gauge, for a monochromatic optical field, we have

$$\mathbf{A}(\mathbf{r},t) = \nabla \times [\psi_e \mathbf{r} + k_0^{-1} \nabla \times (\psi_m \mathbf{r})] \mathrm{e}^{-i\omega t}, \tag{8}$$

where ψ_e and ψ_m are two independent scalar functions that satisfy

$$(\Delta + k^2)[\psi_e, \psi_m] = 0. \tag{9}$$

For a microsphere of radius a, using the natural spherical coordinates system, we may write the general solution of Eq. (9) as

$$\psi_e = \sum_{l=0}^{\infty} \sum_{m=0}^{l} \rho_l^E(r) P_l^m(\cos\theta) \times (A_{lm}^c \cos m\phi + A_{lm}^s \sin m\phi), \tag{10}$$

$$\psi_m = \sum_{l=0}^{\infty} \sum_{m=0}^{l} \rho_l^M(r) P_l^m(\cos\theta) \times (B_{lm}^c \cos m\phi + B_{lm}^s \sin m\phi), \tag{11}$$

in which $P_l^m(z)$ is the associated Legendre function, and

$$\rho_l^E(r) = \begin{cases} g_l^s j_l(k_s r) & r < a \\ h_l^{(2)}(k_0 r) + g_l^0 h_l^{(1)}(k_0 r) & r \geq a \end{cases}, \tag{12}$$

$$\rho_l^M(r) = \begin{cases} f_l^s j_l(k_s r) & r < a \\ h_l^{(2)}(k_0 r) + f_l^0 h_l^{(1)}(k_0 r) & r \geq a \end{cases}. \tag{13}$$

In Eqs. (12) and (13), $j_l(z)$ is the lth order spherical Bessel function, $h_l^{(1)}(z)$ and $h_l^{(2)}(z)$ are the lth order spherical type I and II Hankel functions, respectively. The coefficients g_l^s, g_l^0, f_l^s, and f_l^0 are determined by the boundary conditions at $r = a$.

Let

$$\psi_e^{(-)} = \sum_{l=0}^{\infty} \sum_{m=0}^{l} h_l^{(2)}(k_0 r) P_l^m(\cos\theta) \times (A_{lm}^c \cos m\phi + A_{lm}^s \sin m\phi), \tag{14}$$

and

$$\psi_m^{(-)} = \sum_{l=0}^{\infty} \sum_{m=0}^{l} h_l^{(2)}(k_0 r) P_l^m(\cos\theta) \times (B_{lm}^c \cos m\phi + B_{lm}^s \sin m\phi). \tag{15}$$

According to the definition of the incident wave, we have

$$\mathbf{A}^{(-)}(\mathbf{r},t) = \nabla \times [\psi_e^{(-)} \mathbf{r} + k_0^{-1} \nabla \times (\psi_m^{(-)} \mathbf{r})] \mathrm{e}^{-i\omega t}, \tag{16}$$

for $r \geq a$. The incident wave is determined by the pumping condition. Therefore, when the pumping condition is given, values of the coefficients A_{lm}^c, A_{lm}^s, B_{lm}^c, and B_{lm}^s are determined.

The Q factor can be calculated now, and we obtain

$$Q = \frac{k_0^2 a^2 I_1}{2 I_2}, \tag{17}$$

with

$$I_1 = \frac{n_\mathrm{r}}{n_\mathrm{i}} \sum_{l=1}^{\infty} |g_l^s|^2 \frac{l(l+1)}{2l+1} \mathrm{Im}[-n j_l'(k_s a) j_l(k_s^* a)] \times \sum_{m=1}^{l} (|A_{lm}^c|^2 + |A_{lm}^s|^2) \frac{(l+m)!}{(l-m)!} + \frac{n_\mathrm{r}}{n_\mathrm{i}} \sum_{l=1}^{\infty} |n f_l^s|^2 \frac{l(l+1)}{2l+1} \{\mathrm{Im}[-n j_l'(k_s a) j_l(k_s^* a)] + \frac{2 n_\mathrm{r} n_\mathrm{i} |j_l(k_s a)|^2}{|n k_s a|}\} \times \sum_{m=1}^{l} (|B_{lm}^c|^2 + |B_{lm}^s|^2) \frac{(l+m)!}{(l-m)!}, \tag{18}$$

and

$$I_2 = \sum_{l=1}^{\infty} \frac{l(l+1)}{2l+1} [\sum_{m=1}^{l} (|A_{lm}^c|^2 + |A_{lm}^s|^2 + |B_{lm}^c|^2 + |B_{lm}^s|^2) \frac{(l+m)!}{(l-m)!}]. \tag{19}$$

Numerical calculations are carried out for glass microspheres. The refractive index is taken to be $n_\mathrm{r} = 1.523$[8], and the wavelength λ of the incident optical wave is taken to be 488 nm. We consider firstly the case when the incident wave is a well focused Gaussian beam. The variation of Q factor as a function of the radius of microspheres is presented in Fig. 1. The Q factor increases from zero and oscillates as the radius of microcavities a increases. For microspheres with higher absorption coefficients (higher n_i), the amplitude of this oscillation is reduced at larger a. The difference between the radii corresponding to two adjacent maximums is equal to $\frac{\lambda}{2n_\mathrm{r}}$. The variation of Q factor with the wavelength λ is shown

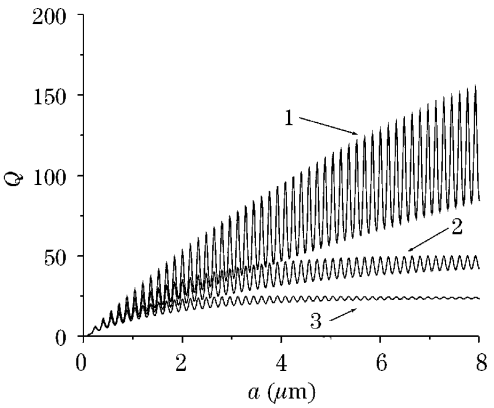

Fig. 1. Variation of Q factor with the radius of spherical microcavities a. The incident wave is a well focused Gaussian beam with $\lambda = 488$ nm. Curve 1: microsphere with refractive index $n = 1.523(1 + 0.001i)$; curve 2: $n = 1.523(1 + 0.005i)$; curve 3: $n = 1.523(1 + 0.01i)$.

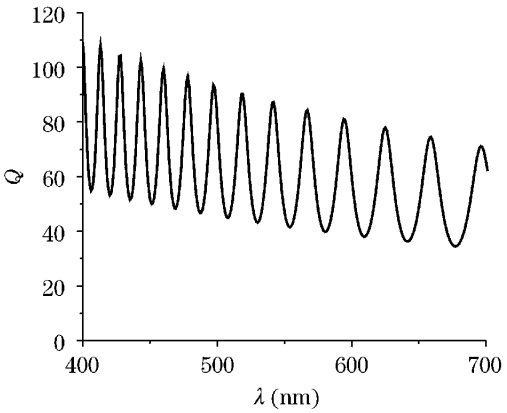

Fig. 2. Variation of Q factor with the wavelength λ. The incident wave is a well focused Gaussian beam. The spherical microcavity's radius $a = 4$ μm, the complex refractive index $n = 1.523(1 + 0.001i)$.

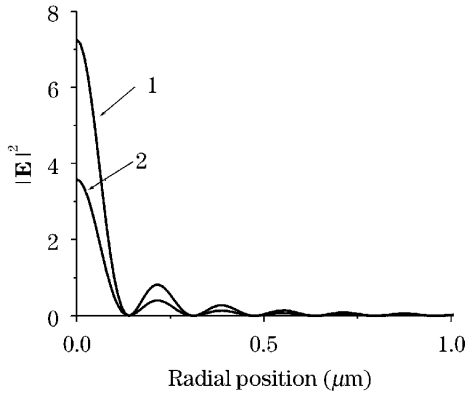

Fig. 3. Distributions of optical field in microspheres. The incident wave is a well focused Gaussian beam. Curve 1: resonating microcavity ($a = 4.25$ μm); curve 2: anti-resonating microcavity ($a = 4.16$ μm).

in Fig. 2. The radius of the microsphere is taken to be 4 μm. Strong oscillations are also found here, that means the incident optical waves are filtered by microspheres.

The radial distributions of the optical field $|\mathbf{E}|^2$ in a resonating ($a = 4.25$ μm) and an anti-resonating microsphere ($a = 4.16$ μm) are illustrated in Fig. 3. The maximal value of $|\mathbf{E}|^2$ in the absence of the microsphere is taken as the unit. In this case, the optical field is strongly confined in the center of the microsphere, and for resonating microspheres, the optical energy intensity could be more than 7 times higher than the case of absence of the microsphere. Therefore using a well focused Gaussian beam as the pumping wave is a suitable choice for experimental cavity quantum electrodynamics studies on spontaneous emission from semiconductor nanocrystals[9] or quantum dots[10] embedded in spherical microcavities.

On the other hand, high Q factor whispering-gallery-modes (WGM) of microspheres are very attractive in manufacturing very low threshold microlasers[11,12]. The optical field of a WGM is mainly distributed near the surface of a microsphere, thus a well focused Gaussian beam is not a suitable pumping source for WGM microsphere lasers. Higher order spherical wave should be used in this case. A lth order spherical wave can be generated by inserting a phase modulator, which divides the section of the pumping wave into $2l$ identical sectors and introduces a phase shift of π or $-\pi$ between two adjacent sectors into the pumping wave.

The variations of Q factor as a function of the radius of microspheres when higher order spherical waves are used as pumping wave are presented in Figs. 4 and 5. The Q factor is significantly different from zero only for microspheres with radii greater than certain critical radii. By comparing Fig. 4 with Fig. 5, one may observe that the value of this critical radius increases with the order of the spherical waves.

The variation of Q factor with the wavelength λ is also calculated for a microsphere with $a = 4$ μm, and illustrated in Fig. 6. We find again the Q factor as an oscillatory function of the radius of a microsphere and the wavelength, but in these cases the differences between the resonating and anti-resonating values of the Q factor are much greater. That means the optical pumping efficiency for a resonating microsphere could be much higher than that for an anti-resonating microsphere. The narrow resonating wavelength bandwidth shown in Fig. 6 suggests that in order to obtain high pumping efficiency, one should use a tunable laser as the optical pumping source.

The radial distributions of the optical field $|\mathbf{E}|^2$ in a resonating ($a = 4.28$ μm) and an anti-resonating microsphere ($a = 4.19$ μm) are shown in Fig. 7. We find in the

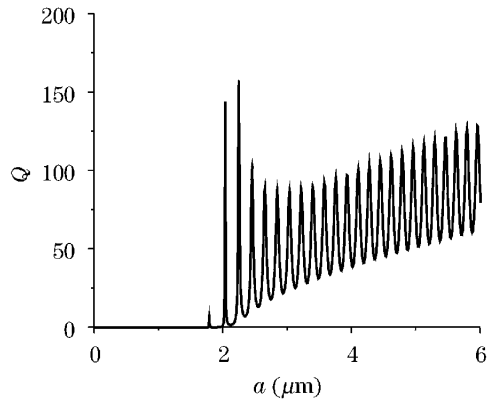

Fig. 4. Variation of Q factor with the radius of spherical microcavities a. The incident wave is a 30th order spherical wave. $\lambda = 488$ nm, $n = 1.523(1 + 0.001i)$.

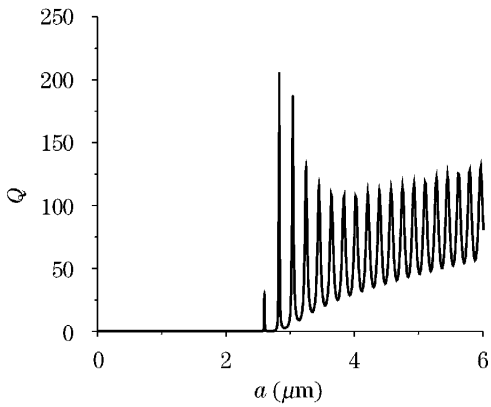

Fig. 5. Variation of Q factor with the radius of spherical microcavities a. The incident wave is a 40th order spherical wave. $\lambda = 488$ nm, $n = 1.523(1 + 0.001i)$.

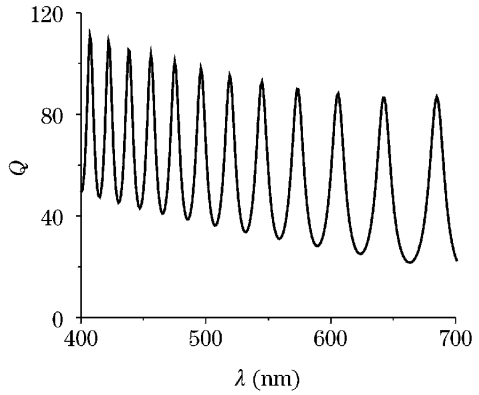

Fig. 6. Variation of Q factor with the wavelength λ. The incident wave is a 30th order spherical wave. $a = 4$ μm, $n = 1.523(1 + 0.001i)$.

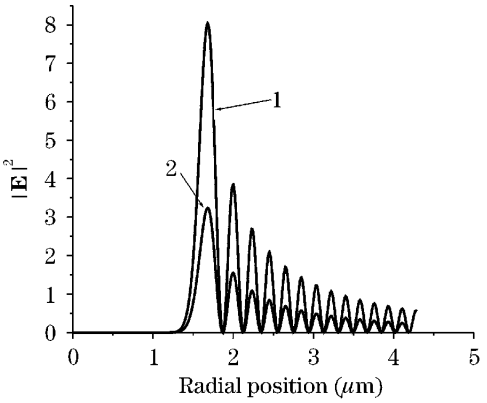

Fig. 7. Distributions of optical field in microspheres. The incident wave is a 30th order spherical wave. $n = 1.523(1 + 0.001i)$. Curve 1: resonating microcavtiy ($a = 4.28$ μm); curve 2: anti-resonating microcavity ($a = 4.19$ μm).

case of a resonating microsphere, the maximal value of the optical energy intensity is 8 times higher than that without the microsphere. We also observe that the optical field intensities in the central region of the microspheres are negligible. A quite large part of the optical energy is distributed near the surface. Thus this mode of incident wave would favor energy transferring to WGM. According to Fig. 9, the modulus of the optical field $|\mathbf{E}|^2$ approaches a local maximum at the surface in the case of resonance, but reaches a local minimum in the case of anti-resonance.

In conclusion, we show that efficiency of the optical pumping process in a microsphere laser depends strongly on its resonating properties as a passive optical cavity. The resonating properties are well described in the terms of the Q factor and the optical field distribution in a microsphere. According to our numerical calculations, the Q factor (and consequently the optical pumping efficiency) is an oscillatory function of the radius of a microsphere and the pumping wavelength. That means the spectrum of the optical field within a microsphere may differ from the spectra of the incident wave, and to achieve a higher pumping efficiency, tunable lasers should be used as pumping sources. Numerical results for optical field distribution in microspheres under different pumping conditions show that using a well focused Gaussian beam as the pumping wave is suitable for cavity quantum electrodynamics experiments where strong confinement of optical field in the center of a microsphere is requested. But for exciting WGM microsphere lasers, higher order spherical wave, which can be generated by inserting a special phase modulator into the pumping wave, should be used. Theoretical analysis and numerical calculations on the resonating property of spherical microcavities presented in this letter could be useful also for microcavities with other geometries[13–15].

This work was supported by the National Natural Science Foundation of China under Grant No. 69977004. R. Wang is the author to whom the correspondence should be addressed, his e-mail address is rpwang@cis.pku.edu.cn.

References

1. D. W. Vernooy, A. Furusawa, N. Ph. Georgiades, V. S. Ilchenko, and H. J. Kimble, Phys. Rev. A **57,** R2293 (1998).
2. W. von Klitzing, R. Long, V. S. Ilchenko, J. Hare, and V. Lefevre-Seguin, Opt. Lett. **26,** 166 (2001).
3. M. J. A. de Dood, L. H. Slooff, A. Polman, A. Moroz, and A. van Blaaderen, Phys. Rev. A **64,** 033807 (2001).
4. V. V. Vassiliev, V. L. Velichansky, V. S. Ilchenko, M. L. Gorodetsky, L. Hollberg, and A. V. Yarovitsky, Opt. Commun. **158,** 305 (1998).
5. K. Sasagawa, K. Kusawake, J. Ohta, and M. Nunoshita, Electron. Lett. **38,** 1355 (2002).
6. Z. L. Gong and C. H. Xu, *Modern Electromagnetic Theory* (in Chinese) (Peking University Press, Beijing, 1990) pp. 248–257.
7. J. D. Jackson. *Classical Electrodynamics* (3rd edition) (John Wiley and Sons, New York, 1999) p. 262.
8. X. Peng, F. Song, S. B. Jiang, N. Peyghambarian, M. Kuwata-Gonokami, and L. Xu, Appl. Phys. Lett. **82,** 1497 (2003).
9. X. D. Fan, M. C. Lonergan, Y. Z. Zhang, and H. L. Wang, Phys. Rev. B **64,** 115310 (2001).
10. R. Jia, D. S. Jiang, P. H. Tan, and B. Q. Sun, Appl. Phys. Lett. **79,** 153 (2001).
11. V. Sandoghdar, F. Treussart, J. Hare, V. Lefevre-Seguin, J.-M. Raimond, and S. Haroche, Phys. Rev. A **54,** R1777 (1996).
12. W. von Klitzing, E. Jahier, R. Long, F. Lissillour, V. Lefevre-Seguin, J. Hare, and S. Haroche, Electron. Lett. **35,** 1745 (1999).
13. G. Z. Wu and B. X. Du, Acta Opt. Sin. (in Chinese) **22,** 563 (2002).
14. J. F. Wu and L. Y. Liu, Acta Opt. Sin. (in Chinese) **22,** 447 (2002).
15. H. D. Zhao and G. D. Shen, Acta Opt. Sin. (in Chinese) **20,** 592 (2000).